Supplementary material for "A comparative isotopic study of the biogeochemical cycle of carbon in modern stratified lakes: the hidden role of DOC"

Robin Havas, Christophe Thomazo, Miguel Iniesto, Didier Jézéquel, David Moreira, Rosaluz Tavera, Jeanne Caumartin, Elodie Muller, Purificación López-García, Karim Benzerara

Supplementary Text

Chlorophyll a peak in the hypolimnion of Alberca de les Espinos

In the main text, discussion part 5.2.3., we discuss the primary production occurring in the hypolimnion of the Mexican lakes. In La Alberca de los Espinos we recorded a peak of chlorophyll a (Chl. a) in the anoxic waters at depths between 15 and 20 m, reaching the same concentrations as in the upper oxygenated waters (Fig. 2). However, this photosynthetic pigment is used as a proxy for oxygenic photosynthesis and thus not usually found in anoxic conditions.

The occurrence of oxygenic organisms in anoxic waters could have several explanations: (i) the Chl. a peak corresponds to a daily vertical migration of phytoplankton, (ii) the distribution of planktonic ecological niches with depth is inherited from the mixing period and did not change despite seasonally implemented stratification of the water column at the time of sampling or (iii) the Chl. a detected by the multi-parameter probe is mistaken with another photosynthetic pigment from anaerobic microorganisms, such as some bacteriochlorophylls which have similar absorption and emission spectra (Taniguchi and Lindsey, 2021 and references therein).

The first two possibilities rely on the presence of cyanobacteria and/or eukaryotic algae under anoxic conditions either as "dormant" forms or active forms with a facultative anaerobic activity. A significant [DOC] increase at the same depth than this Chl. a peak suggests the presence of active organisms releasing DOC in the anoxic waters (~17 m, Fig. 3). Meanwhile, cyanobacteria can be specifically targeted by the phycocyannin pigment and are only found to match the Chl. a peak around 12-13 m (Fig. 2). Besides, unicellular eukaryotic algae do not perform anoxygenic photosynthesis (Atteia et al., 2013). Alternatively, aerobic unicellular photosynthetic eukaryotes forced to anoxic conditions can switch to fermentative metabolism (Atteia et al., 2013) which could participate in the DOC production observed at 17 m depth (Fig. 3). However, their presence in the anoxic waters despite more favorable conditions in shallower oxygenated waters of the lake where green algae thrive (Chl. a peak between 5 and 10 m, Fig. 2) seems unlikely.

Moreover, anoxic waters of stratified water bodies are typical habitats of anoxygenic photosynthesizers such as green or purple sulfur bacteria (GSB and PSB, respectively) (e.g. Fulton et al., 2018). These organisms usually operate in deeper and darker conditions than oxygenic organisms and use photosynthetic pigments different than Chl. a. Namely, GSB synthetize bacteriochlorophyll (BChl.) c, d or e while PSB synthesize BChl. a as their main photosynthetic pigments (Fulton et al., 2018; Hamilton, 2019). Although the molecular composition of these pigments slightly differs from one another, some of them share close optical characteristics with Chl. a. Notably, BChl. c and d and Chl. a share B and Q bands of absorption at around 430 and 660 nm, respectively (see Table 1 in Taniguchi and Lindsey, 2021). Meanwhile BChl. a bands are very distant from these values (~ 360 and 770 nm). Furthermore, BChl c, d and e and Chl. a also share very close fluorescence wavelengths around 670 nm while BChl. a reemits around 790 nm (Table 2 in Taniguchi and Lindsey, 2021). Since the multi-parameter probe that we used detects Chl. a based on these absorption and reemission wavelengths, the probe would most likely confuse Chl. a with BChl. c and d (and possibly BChl. e) which are characteristic pigments of GSB while differentiating well with BChl. a characteristic of PSB.

In conclusion, the third chlorophyll a peak in the anoxic waters of Lake La Alberca could partly be the result of vertical migration of oxygenic photosynthetic organisms, but it more likely represents a bias of the probe towards bacteriochlorophylls pigments typical of green sulfur bacteria, reflecting the presence and activity of anoxygenic phototrophs at these depths.

Calculation of $\delta^{13}C$ signatures from the different DIC species ($CO_{2(aq)}$, HCO_3^-, CO_3^{2-}) from the bulk $\delta^{13}C_{DIC}$

The analytical method of DIC isotopes determination allows to measure the bulk DIC isotopic composition (see method in the main text), integrating the weighted average of $CO_{2(aq)}$, HCO_3^- and CO_3^{2-} respective isotopic compositions such as:

$$\delta^{13}C_{DIC} = ([HCO_3]*\delta^{13}C_{HCO3} + [CO_3]*\delta^{13}C_{CO3} + [CO_2]*\delta^{13}C_{CO2}) / [DIC] , \quad (1)$$

However, strong isotopic fractionations of about 10 ‰ exist between the dissolved $CO_{2(aq)}$ and the two other DIC species (e.g. Mook et al., 1974). At the pH of the studied Mexican lakes (~ 9), $CO_{2(aq)}$ represents less than 0.5 % of total DIC (Table S4). Therefore, its isotopic composition significantly differs from that of the bulk DIC and needs to be calculated *a posteriori* when considering processes involving CO_2 specifically.

We can isolate and calculate $\delta^{13}C_{CO2}$ by using the isotopic fractionation between the different DIC species (α_{X-Y}). The "per mil fractionation" $1000ln\alpha_{X-Y}$ – when around 10 ‰ or less – is almost identical to the isotopic difference between different species ($\Delta^{13}C_{X-Y} = \delta^{13}C_X - \delta^{13}C_Y$) (Sharp, 2017). Therefore, we use $\Delta^{13}C$ to derive Eq. (1) such as:

$$\delta^{13}C_{CO2} = \delta^{13}C_{DIC} - ([HCO_3]*\Delta^{13}C_{HCO3\text{-}CO2} - [CO_3]*\Delta^{13}C_{CO3\text{-}CO2}) / [DIC], \quad (2)$$

We used $\Delta^{13}C$ data from Emrich et al. (1970) who provide isotopic fractionations between all three DIC species as a function of temperature. All temperatures and resulting isotopic fractionations and compositions are summarized in Table S5.

Calculation of the methane $\delta^{13}C$ endmember from the sediment porewaters of Lake La ALberca de los Espinos

In La Alberca de los Espinos, the isotopic composition of DIC strikingly increases from the middle of the lake water column to the first 10 cm of sediment porewaters (Table 2 and S4). This can be well explained by the action of acetoclastic methanogenesis which degrades sedimentary OM to produce ^{13}C-depleted methane and ^{13}C-rich carbon dioxide diffusing upward in the water column (main text part 5.2.4). Following the simplified equation

$$CH_3COOH \rightarrow CO_2 + CH_4 \, , \qquad (3)$$

the C isotopic composition of methane ($\delta^{13}C_{CH4}$) can be calculated by mass balance based on C isotopic compositions of sedimentary OC and dissolved CO_2 ($\delta^{13}C_{SOC}$ and $\delta^{13}C_{CO2}$, respectively) such that:

$$\delta^{13}C_{SOC} = 0.5*\delta^{13}C_{CO2} + 0.5*\delta^{13}C_{CH4} \, , \qquad (4)$$

and thus:

$$\delta^{13}C_{CH4} = 2*\delta^{13}C_{SOC} - \delta^{13}C_{CO2} \, . \qquad (5)$$

Following Eq. (5), we calculate $\delta^{13}C_{CH4}$ at depth where $\delta^{13}C_{SOC}$ and $\delta^{13}C_{CO2}$ are available, *i.e.* at 0.5 and 7 cm depths within the sediments of Lake La Alberca (Table S4).

In this calculation, we consider that the isotopic composition of the sedimentary organic carbon that we measured corresponds to the one used by methanogen organisms. Moreover, we consider that the bulk isotopic composition of porewater DIC ($\delta^{13}C_{DIC}$) is related to methanogenesis. This is supported by the fact that (i) the very positive $\delta^{13}C_{DIC}$ can unequivocally be explained by methanogenesis while differing from the water column $\delta^{13}C_{DIC}$ and (ii) that the DIC concentration gradient between the porewater and the lake water forces the DIC to diffuse from the porewater to the lake water rather than the other way around. Nonetheless, we consider that there is isotopic exchange between the different DIC species of the porewater and lake water (as suggested by the diffusion of DIC through the porewaters and sediment-water interface). Hence, we use the calculated $\delta^{13}C_{CO2}$ value rather than bulk $\delta^{13}C_{DIC}$ in the calculation of Eq. (5).

Numerical derivation of Eq. (5) for depths 0.5 and 7 cm in the sediments are $\delta^{13}C_{CH4}$ = -59.0 ‰ and $\delta^{13}C_{CH4}$ = -56.8 ‰, respectively.

Supplementary Figures

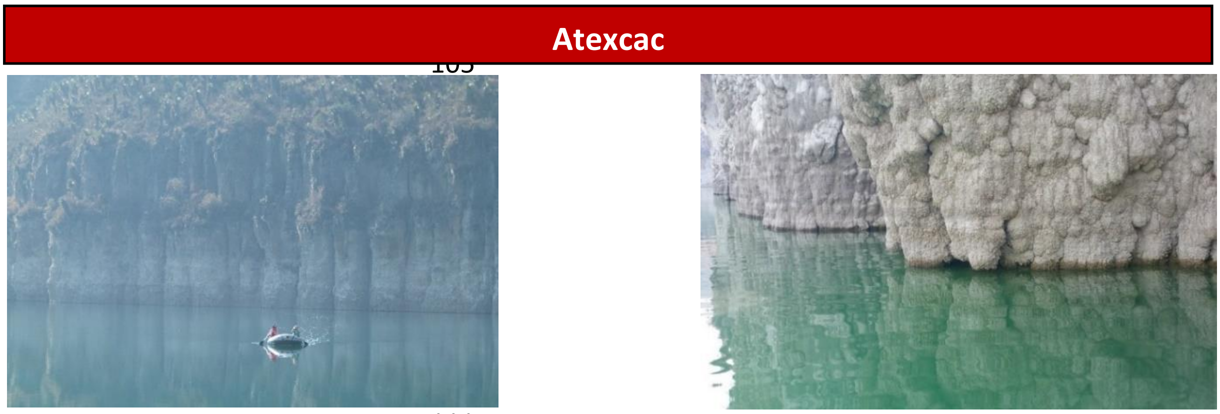

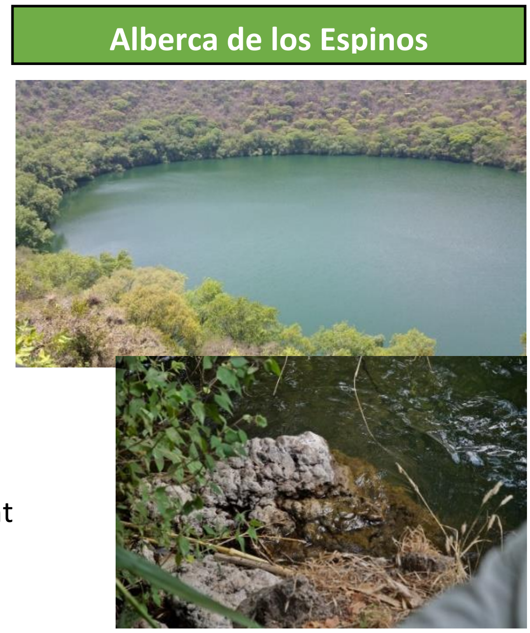

Figure S1. Photographs of the lakes showing different levels of emerged microbialites.

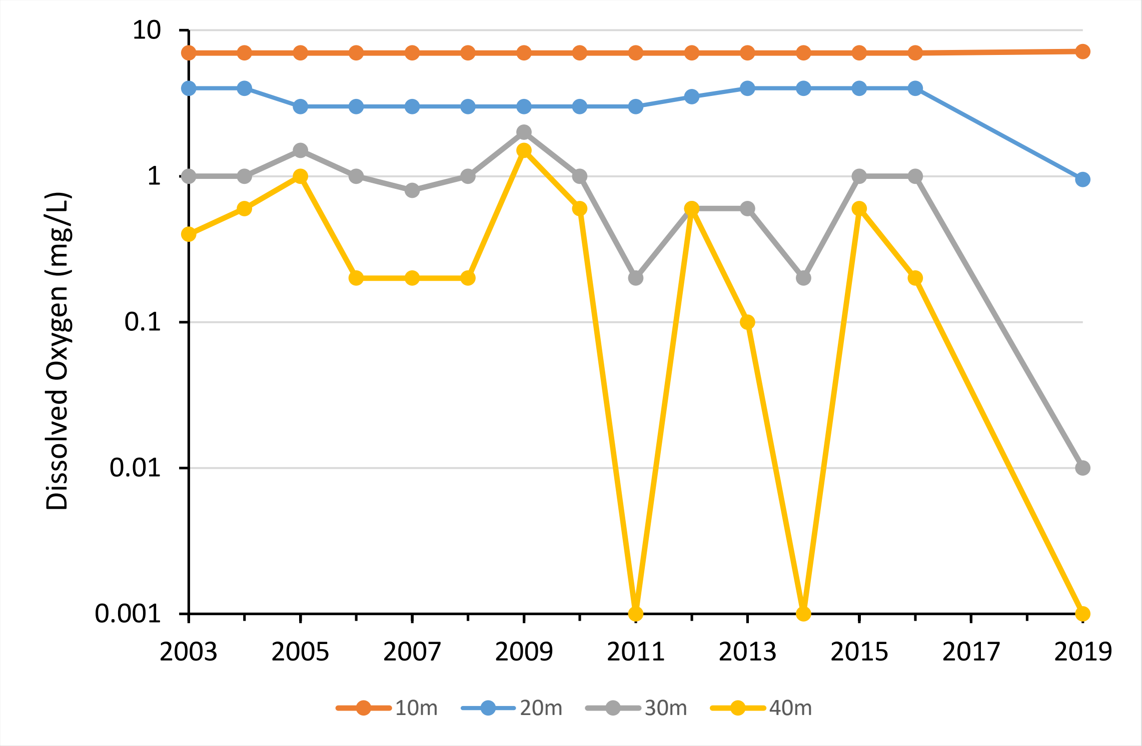

Figure S2. Dissolved oxygen (DO) concentrations in mg/L at 10, 20, 30 and 40m depth in lake Alchichica in May since 2003. Data between 2003 and 2017 from Macek et al., 2020. We notice that DO is lower in 2019 than other years at each depth pointing out the sharper stratification of the lake in 2019.

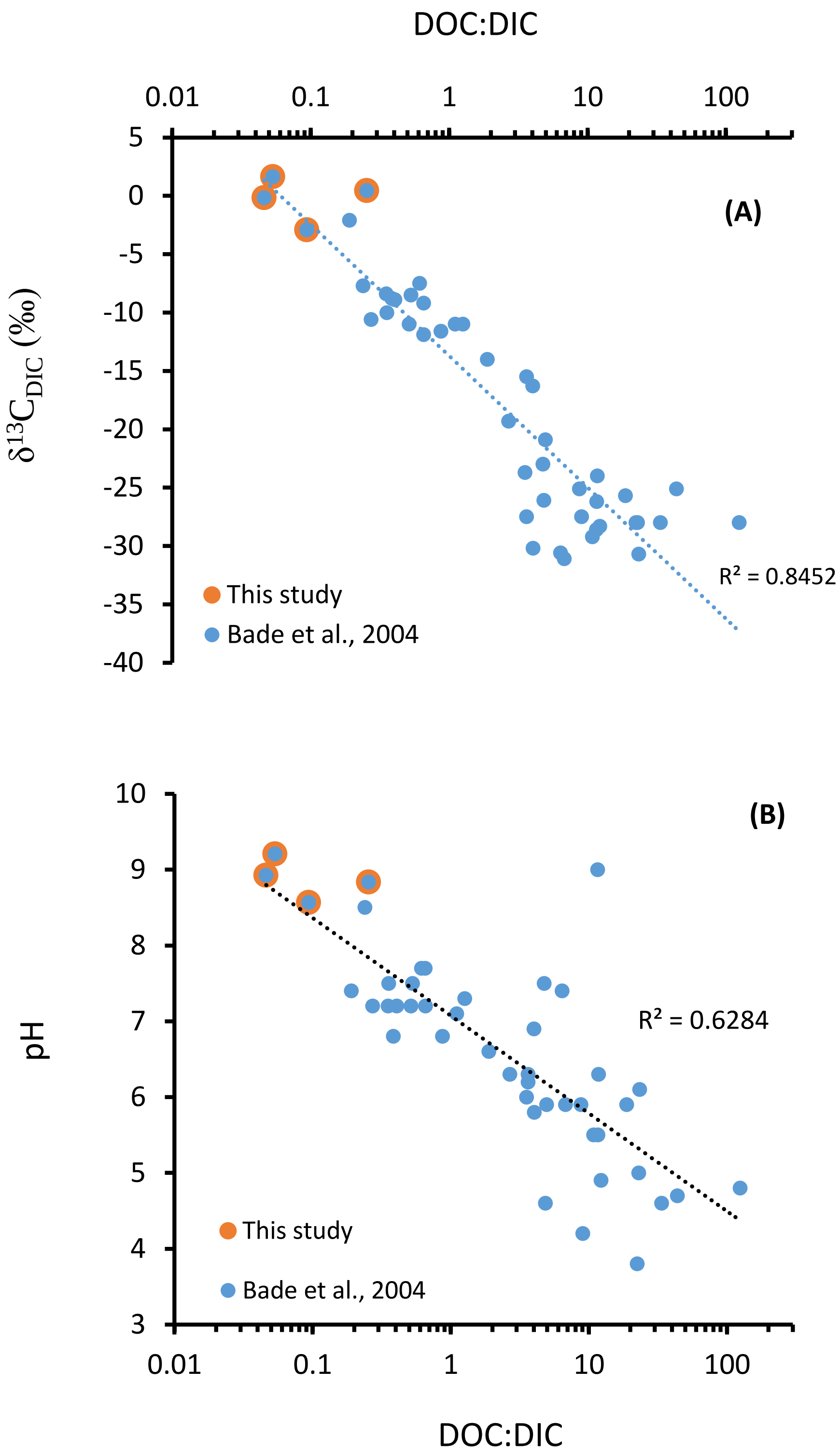

Figure S3. DOC:DIC ratios, pH and $\delta^{13}C_{DIC}$ values from different lakes with values compiled from Bade et al., 2004 and the four Mexican lakes from this study. (A) $\delta^{13}C_{DIC}$ as a function of DOC:DIC ratio represented with a logarithmic x abscises scale and logarithmic trend line and corresponding correlation coefficient R^2. (B) pH as a function of DOC:DIC ratio again logarithmic x abscises and trend line. Most of the dispersion occurring for both graphs results from lakes with low [DIC] < 145 µM.

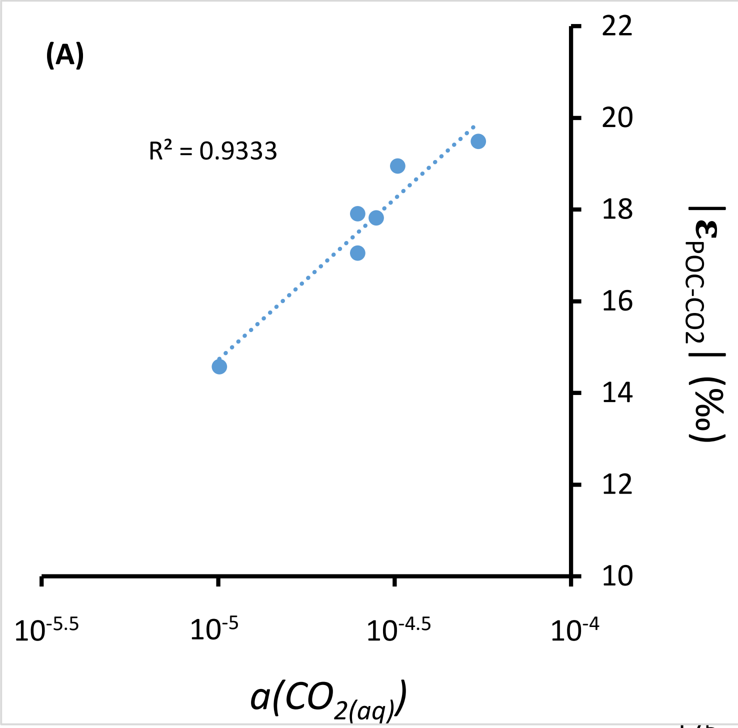

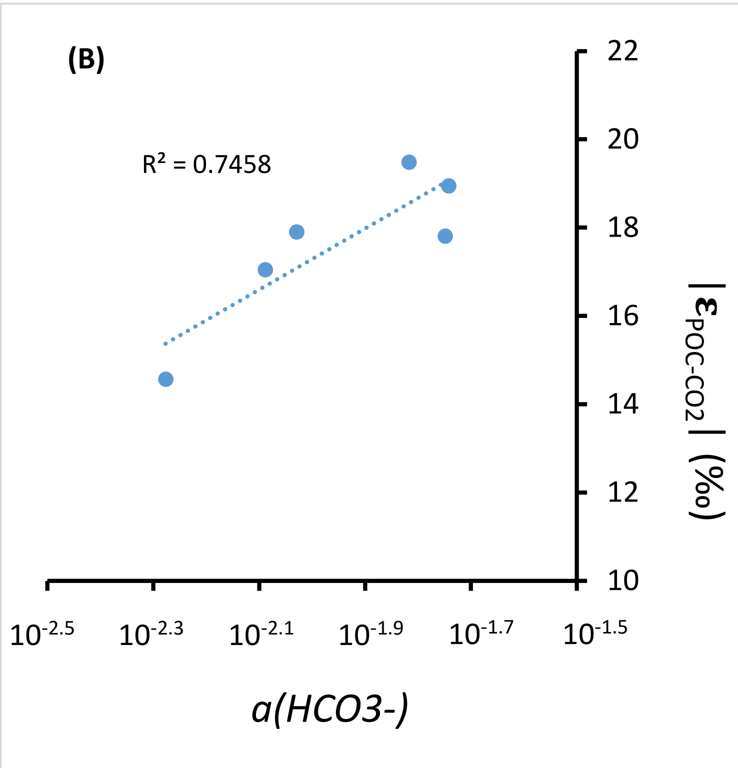

Figure S4. Cross plots of DIC species activities versus absolute values of calculated C isotopic fractionations between POC and CO_2 at depths of peak oxygenic photosynthesis where data was available (5 and 30 m for Alchichica, 16 m for Atexcac, 10 and 12.5 m for La Preciosa and 7m for Alberca). (A) Dissolved $CO_{2(aq)}$ activity and (B) bicarbonate activity as functions of $|\varepsilon_{POC\text{-}CO2}|$ in ‰ plus linear correlation trends and corresponding R^2.

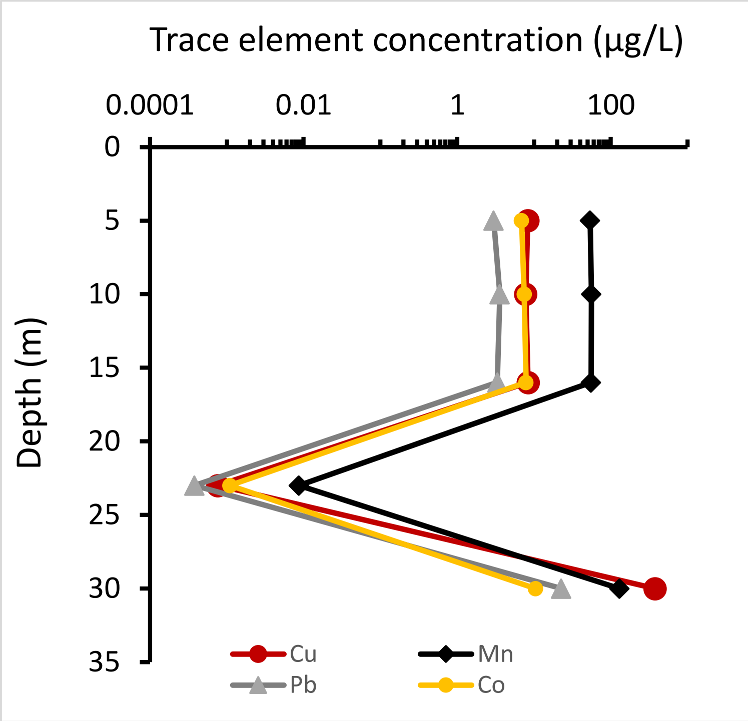

Figure S5. Depth profile of several metal ions dissolved in the waters of Lake Atexcac.

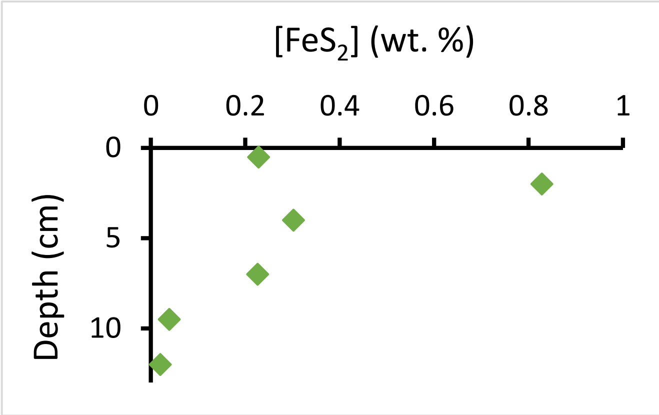

Figure S6. Pyrite concentrations in weight percent in the surficial sediments of Lake La Alberca de los Espinos.

Supplementary Tables

Table S1

Ionic concentrations in the water columns of the four lakes. TDP and TDS stands for ‘total dissolved P’ and S’, respectively, and were measured by ICP-AES. Fe and Mn were measured by ICP-MS. Nitrogen species were measured by colorimetry and Cl^- and SO_4^{2-} by chromatography.

Lake	**Sample**	**TDP**	**NH_4^+**	**Fe**	**Mn**	**SO_4^{2-}**	**TDS**	**Cl^-**
		µmoles/L			mmoles/L			
Alchichica	AL 4.9m	0.3	3.1	0.3	1.4	11.8	10.1	107
	AL 5m	0.4	2.9	0.2	1.5	11.9	10.2	107
	AL 10m	0.4	2.4	0.3	1.7	11.8	10.1	106
	AL 20m	0.5	3.5	0.2	0.4	11.8	10.1	106
	AL 30m	1.6	2.9	0.2	0.4	11.7	10.1	106
	AL 40m	1.8	3.5	0.1	0.5	11.8	10.0	107
	AL 50m	2.5	3.3	<LD	0.4	12.0	10.0	108
	AL 55m	2.6	13.0	<LD	0.5	12.0	9.7	109
	AL 60m	3.2	3.9	0.1	1.0	12.2	10.0	111
Atexcac	ATX 5m	0.3	2.4	0.8	1.0	2.5	2.4	122
	ATX 10m	0.2	2.4	0.7	1.0	2.5	2.4	122
	ATX 16m	0.2	2.5	0.4	1.0	2.5	2.4	121
	ATX 23m	0.4	2.5	0.2	0.0	2.6	2.5	126
	ATX 30m	0.5	2.9	0.1	2.4	2.5	2.4	124
La Preciosa	LP 5m	0.2	1.8	0.1	1.1	1.2	1.2	8.4
	LP 8m	0.2	2.0	<LD	0.3	1.2	1.2	8.2
	LP 10m	0.2	1.6	<LD	0.4	1.2	1.2	8.0
	LP 12.5m	0.2	1.4	<LD	0.4	1.2	1.2	7.8
	LP 15m	<LD	2.0	<LD	0.6	1.2	1.2	7.9
	LP 20m	0.3	2.3	<LD	1.4	1.2	1.2	7.9
	LP 30m	0.3	2.2	<LD	1.0	1.2	1.2	7.9
La Alberca de Los Espinos	Albesp 5m	2.9	2.4	<LD	1.5	0.012	0.009	4.2
	Albesp 7m	3.0	3.1	<LD	0.8	<LD	0.008	4.2
	Albesp 10m	7.6	3.5	<LD	0.5	<LD	0.006	4.0
	Albesp 17m	11.0	2.5	<LD	0.6	<LD	0.009	4.0
	Albesp 20m	15.6	8.5	<LD	1.0	<LD	0.008	4.2
	Albesp 25m	27.4	3.3	0.2	1.9	<LD	0.013	4.2

Table S2.

Surficial solid sediment and pore water analyses: C:N ratio and C isotopic composition of sedimentary organic matter and carbon (SOM, SOC), concentrations and isotopic compositions of DIC in the pore waters.

Lake	**Sample name**	**Depth**	**$(C:N)_{SOM}$**	**$\delta^{13}C_{SOC}$**	**DIC**	**$\delta^{13}C_{DIC}$**
		cm	(molar)	‰	mmoles/L	‰
Alchichica	**AL19_C2a_01**	0-1	10.4	-25.7	35.8	0.4
	AL19_C2a_02	1-3	10.2	-25.7	36.2	0.0
	AL19_C2a_03	3-5	ND.	-25.3	36.8	-0.1
	AL19_C2a_04	5-7	10.4	-25.1	34.5	-0.3
	AL19_C2a_05	7-10	10.4	-24.6	34.6	-0.4
	AL19_C2a_06	10-13	10.4	-24.5	34.9	-0.5
Atexcac	**ATX19_C1_1**	0-1	8.2	-26.7	24.4	0.3
	ATX19_C1_2	1-2	7.9	-26.8	22.5	-0.2
	ATX19_C1_3	2-4	8.0	-26.8	20.7	0.4
	ATX19_C1_S4	4-7	8.6	-27.0	ND.	ND.
	ATX19_C1_4	7-9	ND.	-26.8	22.7	0.5
	ATX19_C1_5	9-10	9.3	-26.9	23.1	0.5
	ATX19_C1_S6	10-12	9.6	-27.0	25.7	0.0
La Preciosa	**LP16_C3_7**	0-2	9.8	-25.1	ND.	ND.
	LP16_C3_8	2-4	9.6	-25.8	ND.	ND.
	LP16_C3_9	8-10	11.0	-23.2	ND.	ND.
La Alberca de Los Espinos	**ALBESP19_C3_1**	0-1	13.1	-28.6	11.2	9.4
	ALBESP19_C3_2	1-3	12.3	-29.4	ND.	ND.
	ALBESP19_C3_3	3-5	11.8	-29.2	ND.	ND.
	ALBESP19_C3_4	5-9	11.6	-27.9	11.9	7.7
	ALBESP19_C3_S5	9-10	14.3	-25.7	ND.	ND.
	ALBESP19_C3_5	10-14	13.5	-25.4	ND.	ND.

Table S3

Iron, sulfur and manganese concentrations in the particulate matter, measured with ICP-AES. <LD = below detection limits.

Lake	Sample	Fe	S	Mn
		10^3*µmoles/L		
Alchichica	AL 4.9m	178	3426	7
	AL 30m	61	1224	3
	AL 35.6m	64	1631	<LD
	AL 40.6m	47	1630	0.2
Atexcac	ATX 5m	821	1624	15
	ATX 10m	973	2486	21
	ATX 16m	368	1195	20
La Preciosa	LP 5m	295	553	70
	LP 8m	236	575	52
	LP 10m	305	525	76
	LP 12.5m	390	661	108
	LP 15m	194	452	124
La Alberca de Los Espinos	Albesp 5m	25	57	29
	Albesp 7m	26	50	28
	Albesp 10m	20	68	63
	Albesp 17m	24	97	1173
	Albesp 20m	230	90	996
	Albesp 25m	5974	561	156

Table S4

Calculated activities of the different dissolved inorganic carbon species, CO_2 partial pressure (P_{CO2}), ratio of P_{CO2} with atmospheric P_{CO2} at 2320m altitude and pH presented for waters at different depths in 2019 and surface waters of years 2012, 2014 and 2018.

Lake	Sample	$a(CO_{2(aq)})$	$a(HCO_3^-)$	$a(CO_3^{2-})$	P_{CO2}	P_{CO2} / $P_{CO2-atm}$	pH
		LOG10			LOG10 (atm)		
Alchichica	**AL 5m**	-4.49	-1.74	-2.98	-3.02	3.1	9.14
	AL 10m	-4.61	-1.79	-2.95	-3.14	2.4	9.22
	AL 20m	-4.57	-1.75	-2.93	-3.10	2.6	9.23
	AL 30m	-4.55	-1.75	-2.95	-3.08	2.7	9.22
	AL 40m	-4.57	-1.75	-2.93	-3.10	2.6	9.24
	AL 50m	-4.48	-1.73	-2.98	-3.01	3.2	9.17
	AL 55m	-4.49	-1.73	-2.97	-3.02	3.1	9.18
	AL 60m	-4.59	-1.76	-2.93	-3.12	2.5	9.25
Atexcac	**ATX 5m**	-4.30	-1.83	-3.35	-2.83	4.9	8.85
	ATX 10m	-4.30	-1.83	-3.36	-2.83	4.9	8.85
	ATX 16m	-4.26	-1.82	-3.37	-2.79	5.3	8.85
	ATX 23m	-4.26	-1.85	-3.45	-2.79	5.4	8.82
	ATX 30m	-4.23	-1.83	-3.43	-2.76	5.7	8.82
La Preciosa	**LP 5m**	-4.67	-2.04	-3.40	-3.20	2.1	9.02
	LP 8m	-4.66	-2.04	-3.41	-3.19	2.1	9.01
	LP 10m	-4.60	-2.03	-3.45	-3.13	2.4	8.97
	LP 12.5m	-4.60	-2.09	-3.57	-3.13	2.4	8.92
	LP 15m	-4.49	-2.02	-3.55	-3.02	3.2	8.88
	LP 20m	-4.48	-2.02	-3.55	-3.01	3.2	8.88
	LP 31m	-4.48	-2.02	-3.56	-3.01	3.2	8.88
La Alberca de Los Espinos	**Albesp 5m**	-5.06	-2.30	-3.53	-3.59	0.9	9.12
	Albesp 7m	-5.00	-2.28	-3.54	-3.53	1.0	9.09
	Albesp 10m	-4.58	-2.23	-3.88	-3.11	2.6	8.73
	Albesp 17m	-4.53	-2.23	-3.93	-3.06	2.9	8.7
	Albesp 20m	-3.88	-2.18	-4.47	-2.41	12.7	8.11
	Albesp 25m	-3.40	-2.15	-4.89	-1.93	38.6	7.66

Lake	**0 m Month-Year**	$a(CO_{2(aq)})$	$a(HCO_3^-)$	$a(CO_3^{2-})$	P_{CO2}	P_{CO2} / $P_{CO2-atm}$	pH
Alchichica	may-14	-4.25	-1.62	-2.98	-2.78	5.4	9.02
	jan-12	-4.28	-1.62	-2.97	-2.81	5.0	9.08
Atexcac	may-14	-3.77	-1.70	-3.62	-2.30	16.5	8.45
	jan-12	-4.07	-1.74	-3.40	-2.60	8.2	8.75
La Alberca	may-14	-4.52	-2.21	-3.89	-3.05	2.9	8.67
La Preciosa	may-14	-4.34	-1.98	-3.61	-2.87	4.4	8.75
	jan-12	-4.46	-1.99	-3.52	-2.99	3.3	8.88
	march-18	-5.14	-2.71	-4.27	-3.67	0.7	8.83

Table S5

Isotopic fractionations between the different DIC species according to the temperature at different depths in the water columns; calculated based on fractionation equations by Emrich et al., 1970.

Lake	Sample	Temperature	$\Delta^{13}C_{HCO3-CO2(aq)}$	$\Delta^{13}C_{CO3-CO2(aq)}$	$\delta^{13}C_{CO2(aq)}$
		°C	‰		
Alchichica	**AL 5m**	19.2	9.7	11.5	-7.7
	AL 10m	18.9	9.7	11.6	-7.8
	AL 20m	16.3	10.0	12.0	-8.5
	AL 30m	15.5	10.1	12.1	-8.5
	AL 40m	15.3	10.1	12.1	-8.7
	AL 50m	15.2	10.1	12.1	-8.6
	AL 55m	15.2	10.1	12.1	-8.7
	AL 60m	15.2	10.1	12.1	-8.7
Atexcac	**ATX 5m**	20.1	9.5	11.4	-9.2
	ATX 10m	19.7	9.6	11.4	-9.1
	ATX 16m	17.2	9.9	11.8	-9.5
	ATX 23m	15.7	10.1	12.1	-9.1
	ATX 30m	15.6	10.1	12.1	-9.8
La Preciosa	**LP 5m**	19.5	9.6	11.5	-9.5
	LP 8m	19.0	9.7	11.6	-9.5
	LP 10m	18.3	9.8	11.7	-9.5
	LP 12.5m	17.0	9.9	11.9	-10.0
	LP 15m	16.2	10.0	12.0	-10.3
	LP 20m	15.6	10.1	12.1	-10.4
	LP 31m	15.4	10.1	12.1	-10.4
La Alberca de Los Espinos	**Albesp 5m**	22.8	9.2	11.0	-11.8
	Albesp 7m	22.1	9.3	11.1	-11.7
	Albesp 10m	19.6	9.6	11.5	-13.6
	Albesp 17m	17.4	9.9	11.8	-13.1
	Albesp 20m	16.9	9.9	11.9	-12.9
	Albesp 25m	16.7	9.9	11.9	-11.3

References

Atteia, A., van Lis, R., Tielens, A.G. and Martin, W.F.: Anaerobic energy metabolism in unicellular photosynthetic eukaryotes. (BBA)-Bioenergetics, 1827, 210-223. https://doi.org/10.1016/j.bbabio.2012.08.002 , 2013.

Bade, D.L., Carpenter, S.R., Cole, J.J., Hanson, P.C., Hesslein, R.H.: Controls of δ^{13}C-DIC in lakes: Geochemistry, lake metabolism, and morphometry. Limnol. Oceanogr. 49, 1160–1172. https://doi.org/10.4319/lo.2004.49.4.1160 , 2004.

Emrich, K., Ehhalt, D.H., Vogel, J.C.: Carbon isotope fractionation during the precipitation of calcium carbonate. Earth Planet. Sci. Lett. 8, 363–371. https://doi.org/10.1016/0012-821X(70)90109-3 , 1970.

Fulton, J.M., Arthur, M.A., Thomas, B., Freeman, K.H.: Pigment carbon and nitrogen isotopic signatures in euxinic basins. Geobiology 16, 429–445. https://doi.org/10.1111/gbi.12285 , 2018.

Hamilton, T.L.: The trouble with oxygen: The ecophysiology of extant phototrophs and implications for the evolution of oxygenic photosynthesis. Free Radical Biology and Medicine, 140, 233-249. https://doi.org/10.1016/j.freeradbiomed.2019.05.003 , 2019.

Macek, M., Medina, X.S., Picazo, A., Peštová, D., Reyes, F.B., Hernández, J.R.M., Alcocer, J., Ibarra, M.M., Camacho, A.: Spirostomum teres: A Long Term Study of an Anoxic-Hypolimnion Population Feeding upon Photosynthesizing Microorganisms. Acta Protozool. 59, 13–38. https://doi.org/10.4467/16890027AP.20.002.12158 , 2020.

Mook, W.G., Bommerson, J.C., Staverman, W.H.: Carbon isotope fractionation between dissolved bicarbonate and gaseous carbon dioxide. Earth Planet. Sci. Lett. 22, 169–176. https://doi.org/10.1016/0012-821X(74)90078-8 , 1974.

Sharp, Z.: Principles of stable isotope geochemistry. https://doi.org/10.25844/h9q1-0p82 , 2017.

Taniguchi, M. and Lindsey, J.S.: Absorption and fluorescence spectral database of chlorophylls and analogues. Photochemistry and Photobiology, 97, 136-165. https://doi.org/10.1111/php.13319 , 2021.